Global Oceans 2021: San Diego - Porto

High Precision Open Laboratory 3D Positioning System for Automated Underwater Measurements

Fabian John*, Sven Ole Schmidt*, Horst Hellbrück*†
*Technische Hochschule Lübeck, Germany
Department of Electrical Engineering and Computer Science, Center of Excellence CoSA
Email: fabian.john@th-luebeck.de, sven.ole.schmidt@th-luebeck.de, horst.hellbrueck@th-luebeck.de
† University of Luebeck, Germany, Institute of Telematics

***Abstract*—Underwater measurements in a lab environment are challenging, with sensors or objects that need to be positioned precisely and reproducible. Existing systems are expensive, often not suited for underwater usage, and not flexible. Underwater's main challenges are determining the "exact" relative position and a positioning system that is operated reliably in a wet environment. The commercial systems available are fixed in dimensions and cannot be fitted to lab conditions. We present our open solution, which is scalable and flexible to be adapted to other applications. The solution consists of a table with readily adaptable components such as positioning components integrated into an MQTT environment with precise stepper motor units. The table is easy to adapt in size, and we take care of special placement for electrical components to not get into contact with water. The system achieves a noticeable performance and is fully automated. The speed is adaptable between $1\ \mathrm{mm/s}$ and $30\ \mathrm{mm/s}$, with a resolution of $0.1\ \mathrm{mm}$.**

***Index Terms*—Positioning, XYZ, Underwater, Laboratory, Arduino, GRBL, MQTT**

I. Introduction

Various research work in the field of communication systems demands a precise positioning of elements in the measurement setup. In the work presented here, an object location is conceivable, where the effect of a disturbance is to be evaluated depending on its exact distance or position. The position and the orientation of the devices, significantly influence the measurement results, so a credible evaluation is only achieved with a precise positioning system. This precise placement also enables the repeatability of measurements like for localization with electro-impedance-tomography (EIT) or ultrasonic systems [1], [2], [3], [4].

For research, we see a demand for precise positioning of measurement systems and objects in underwater laboratory environments, such as the water tank shown in Figure 1. For this, we strive for a system that can be adopted mechanically and provides automation for the measurement task so that no human interaction is involved and reproducibility is given. Also, we demand a certain flexibility for scaling in size, speed, and resolution, while the system's structure is still cost- and space-efficient. We need open communication interfaces for the positioning system to achieve a high degree of automation in scientific measurements. This is a challenge because commercially available laboratory positioning systems or reference designs from other researchers fulfilling all demands are rarely designed for wet environments [5].

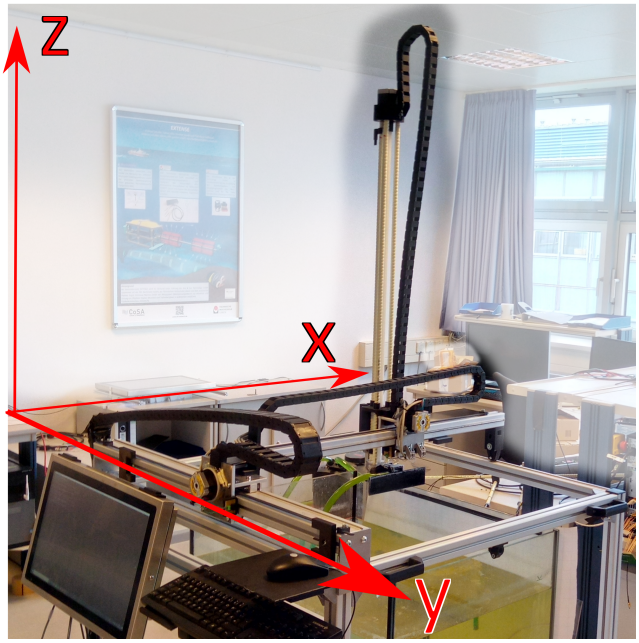

Figure 1: Scalable laboratory 3D positioning system for underwater measurements.

Global Oceans 2021: San Diego - Porto

As a solution, we present a new design of a high-precision 3D positioning system for water tanks for a laboratory environment. Since the sensor nodes are placeable in a range of $80\ \mathrm{cm} \times 90\ \mathrm{cm} \times 90\ \mathrm{cm}$ we achieve a precision of $0.0741\ \mathrm{mm}$ and repeatability of $0.064\ \mathrm{mm}$ for each measurement. The interface for control is connected to a TCP/IP-based Message Queuing Telemetry Transport (MQTT)-system, which enables the open access to an unlimited number of users, if needed [6], [7], [8].

The system is open for use by other researchers and can be easily adapted and scaled to their laboratory environments from our reference design. We offer download of the CAD models of our positioning system, including adapters for stepper units, adaptable end-position switches, and other components, links on our project repository[1]. The primary focus was on the choice of non-conductive materials for system components conducted to the water so that measurements with magnetometers or electro-impedance-tomography [1], [9] are not disturbed by the mechanical setup.

The contributions of the paper are:

- We present a complete 3D positioning system with mechanical, electrical, and software components for a scalable, high precision underwater applications based on open technologies.
- We integrate the positioning system into an automated measurement system.
- We evaluate the precision and repeatability of the positioning system with a laser reference system.

The paper structures as follows. First, we describe the design and implementation of our 3D positioning system in terms of mechanical hardware, electrical components, and software. We show the integration of the positioning system into an automated flexible measurement system. We describe the measurement setup to evaluate the precision and repeatability of our positioning system and show the results. Finally, we summarize the results of our work and give an outlook for the future.

II. Implementation

The complete laboratory 3D positioning system, with a water-filled tank, electrical cabinet, panel PC, and table with XYZ-stepper units, is shown in Figure 1. In this section, we describe the implementation of our positioning system, starting with the mechanical components in Section II-A, followed by the electrical implementation and interfaces in Section II-B, and the firmware and software components.

A. Mechanical Construction

We mount the portable positioning components on a slightly higher frame than the water-filled tank because we have to apply it from the top side. The electrical components of the positioning system are located outside and above the water and do not require increased water tightness requirements to use cost-efficient parts. The positioning system consists of two gliders, which move on rails as a cross table in the X and Y direction with belt drive (see Figure 2).

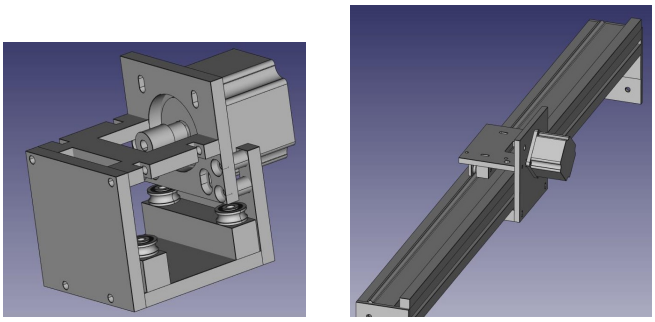

(a) Glider with stepper motor adaption. (b) Rail mounted glider.

Figure 2: X-axis construction.

The positioning in the Z direction is realized by a spindle drive, with a stepper motor mounted on top. The Z-axis has attached to the glider of the X-axis of the cross table so that the Z-axis's stepper motor is always above the X-axis glider. We designed and printed a mounting component (PLA) on the bottom of the Z-axis to adapt varying sensors or objects with a 3D Printer. The adaptation of the Z-axis to the X-axis glider is shown in Figure 3b, the adapter for the stepper motor in Figure 3a and the mounting component in Figure 3c. A spindle made of plastic (PVC) runs through the center of the three components, and three probation rods made of glass fiber are guided through the outer three guides for stabilization.

On each of the axes, two light barriers were installed as end-positions for collision avoidance. The modules for interrupting the light barrier can be mounted variably along the axis, and these also form a mechanical stop if the function of the light barrier is disturbed. A mounted module for interrupting the light barrier is shown in Figure 4. The light barrier is interrupted by the centered bar, before the glider hits the bars at the top and the bottom, in case of a faulty light barrier.

Our mechanical design is scalable in size for all axes. By using the groove profiles, the design is very modular and easily expandable to other laboratory conditions.

B. Electrical Setup

Three stepper motors drive the gliders of the 3D positioning system in the X, Y, and Z directions. Each stepper is connected

[1]https://git.mylab.th-luebeck.de/fabian.john/lab-xyz-pos-system.git

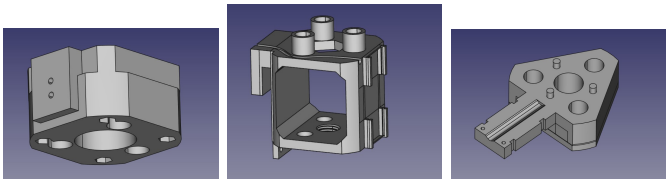

(a) Z-axis motor adapter at the top. (b) Z-axis adaption to the X-axis glider. (c) Mounting component at the Z-axis bottom.

Figure 3: Z-axis components.

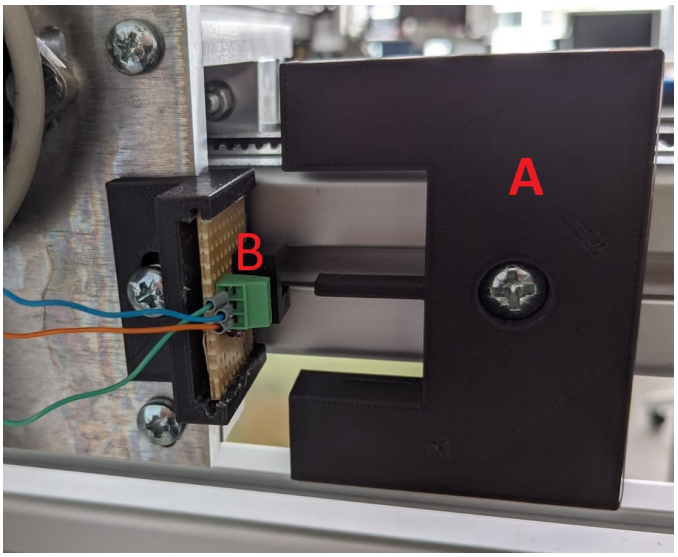

Figure 4: Mechanical end-position with light barrier interruption (A) and light barrier (B) mounted on a glider.

to an Arduino via a stepper motor driver. Furthermore, light barriers are attached to the gliders as end-position switches to prevent collisions (see Figure 4).

TABLE I: Components of the positioning system.

Parameter	**Value**
Stepper motor	ACT 23HS5420 Nema 23
Stepper driver	ACT DM420
Light barriers	Everlight ELITR9809
Power Supply	Meanwell DRP 240-24
Control PC (Panel PC)	
CPU	Intel(R) Core(TM) i7-6500U @2.5 GHz
RAM	16 GB
Network	2×1 GBit
OS	64 Bit Windows 10
Arduino Mega 256	
CPU	ATmega2560
SRAM	8 KB

The Arduino, the stepper motor drivers, and a 24 V power supply are installed in a control cabinet at the frame as shown in Figure 1. A waterproof Panel PC is connected to the power supply and Arduino in the control cabinet. The components are listed in Table I. For the electrical circuit diagram, we refer to documentation in our project repository[2].

C. Firmware and Software

The stepper motors are controlled via the drivers by GPIO channels of the Arduino with GRBL[3]. The Arduino is connected to the control computer (panel PC) via a serial interface. The positioning system is controlled either by a graphical user interface (GUI) or remotely via MQTT protocol on the panel PC with Python software programmed in Python.

The positioning system can approach either absolute position data, related to a user-defined origin, or relative position data. The acceleration and deceleration ramps for starting and stopping are set, for example, via our GUI software. In addition, the travel speeds, steps per revolution, or steps per mm are also set via the GUI. We also make our GUI and MQTT-based remote software available for use through our project repository.

III. Evaluation

A. Precision

We performed a measurement to determine the precision of our positioning system with a laser distance measurement system (Keyence IL100) attached to the frame. This measurement system provides sufficient measurement accuracy with $4\ \mu\mathrm{m}$ repeatability [10]. The measurement range of the laser distance measurement system is from $80\ \mathrm{mm}$ to $120\ \mathrm{mm}$ [10]. The analog measurement result of the laser was acquired automatically via MQTT by a RedPitaya, an embedded signal processing device [6], [11].

To measure the precision of our system, it was first moved to a position P_{ref} within the measurement range of the laser measurement system. The position was changed in steps of $0.1\ \mathrm{mm}$ in the X direction away from the laser measurement system. At each position the distance to the laser was read out 100 times and the mean distance d and the standard deviation σ were calculated from the measurements.

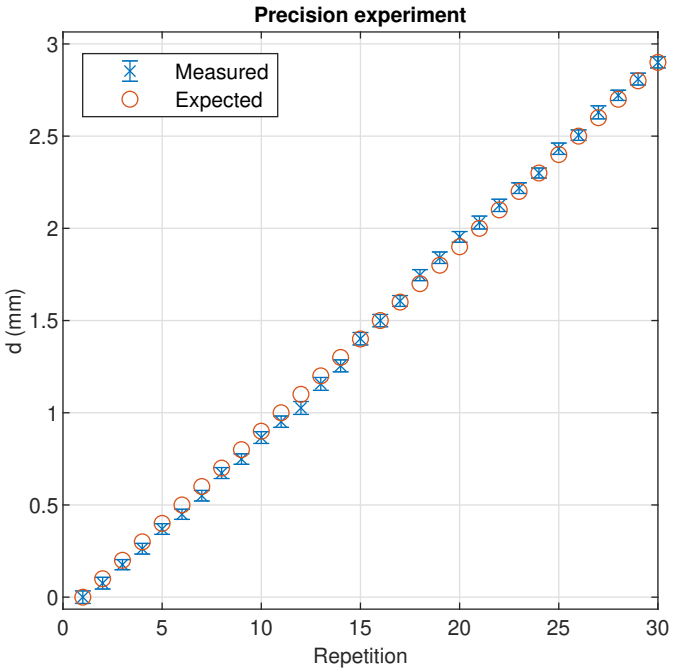

Figure 5: Measurement results for the determination of the positioning system's precision.

[2]https://git.mylab.th-luebeck.de/fabian.john/lab-xyz-pos-system.git
[3]https://github.com/gnea/grbl-Mega

Global Oceans 2021: San Diego - Porto

Figure 5 shows measured and expected distances to the laser measurement system. On average, the precision was calculated as $0.0286\ \mathrm{mm}$ and is maximum $0.0741\ \mathrm{mm}$.

B. Repeatability

To measure the repeatability of our system, it was first moved to a position P_{ref} within the measurement range of the laser measurement system. This position, at the beginning of the measurements, serves as a reference position in the measurement process, and the distance to laser measurement system d_{ref} was determined first. In the progress of the measurement, our positioning system was moved to a new spatial position P_{motion} with relative positioning. Subsequently, the system was moved back to the reference position by the same relative distance. Arriving at the reference position, the distance d to the laser measurement system was measured after a pause of $5\ \mathrm{s}$ to allow oscillations to decay after the movement. We performed the measurement 100 times to calculate the mean distance $\overline{d}$ and standard deviation σ for a position. The deviation of the measured position from the reference position was determined by Equation 1.

$$\Delta d = \overline{d}_{\text{ref}} - \overline{d} \tag{1}$$

The measurement of repeatability was performed with a number of experiments that differ in their motion. Each experiment was repeated 50 times to provide statistically sound measurement of the repeatability and to detect drifts of the reference position if they occur. The motions for the experiments are given in Table II.

TABLE II: Motion for experiments of the repeatability measurement.

#	P_{motion} (x, y, z)
1	(-10, 0, 0)
2	(0, -10, 0)
3	(0, 0, 10)
4	(-10, -10, 0)
5	(-10, -10, 10)
6	(-100, 0, 0)
7	(-200, -200, 20)

Figure 6 shows the calculated deviation Δd from the reference position and the standard deviation σ to the reference distance $\overline{d}_{\text{ref}}$ for each measurement performed. Noise in the measurement chain leads to deviations of the respective measurement positions $\overline{d}$ and were quantified with a standard deviation $\sigma \approx 0.03\ \mathrm{mm}$. The deviations Δd during the repetition of the experiments (except for experiment 3) are within the measurement noise. The average deviation $\overline{\Delta d}$ and the maximum deviation $d_{\text{abs,max}}$ for each experiment are given in Table III.

With free space positioning in all orientations, we determine the repeatability of our positioning system with the maximum deviation (for experiment 3) as $0.064\ \mathrm{mm}$. When moving the Z-axis, the most significant deviations occur due to the large manufacturing tolerances of the PVC spindle. In our

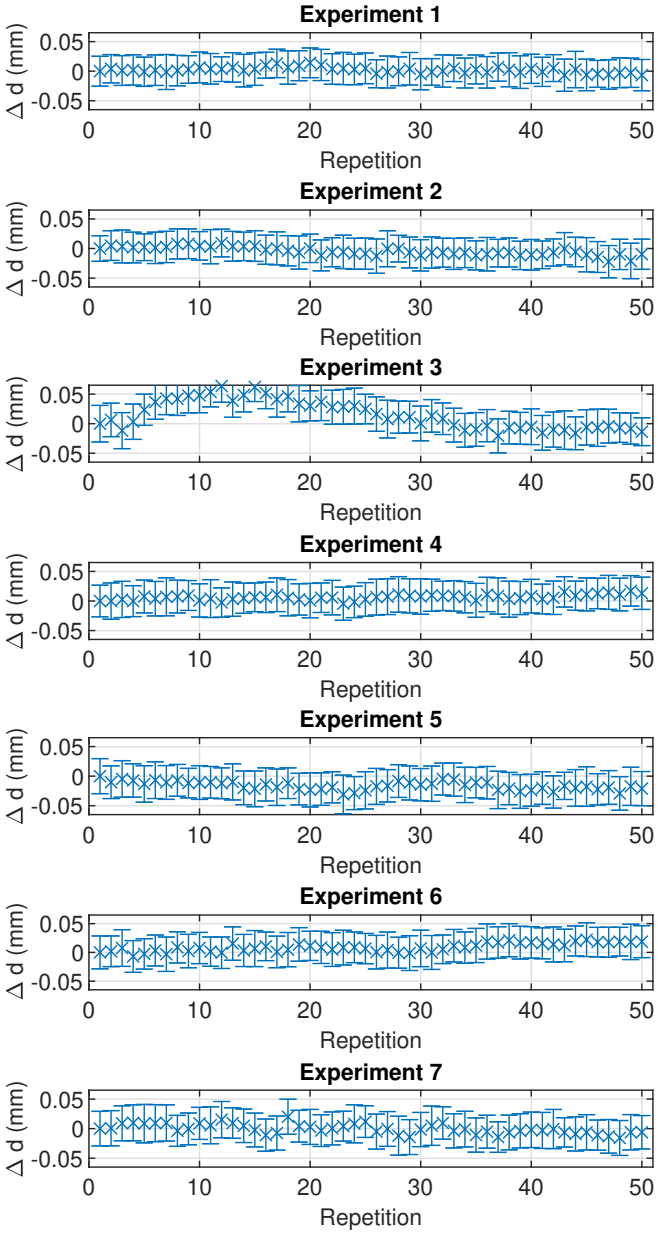

Figure 6: Measurement results for all experiments.

TABLE III: Mean deviation $\overline{\Delta d}$ and maximum absolute deviation $\Delta d_{\text{abs,max}}$ for each experiment.

#	$\overline{\Delta d}$ in mm	$\Delta d_{\text{abs,max}}$ in mm
1	0.0019	0.01412
2	-0.0045	**0.0223**
3	0.0152	**0.0637**
4	0.0062	0.0172
5	-0.0160	0.0309
6	0.0087	0.0221
7	-0.0006	0.0201

setup, a spindle made of electrically and magnetically inactive material was required so that, for example, EIT and magnetic measurement methods are less affected by the components of the positioning system. With an improved spindle (e.g., made of stainless steel as used by 3D printers), we expect a significantly better repeatability and precision.

For tests in which the position of the Z-axis is not varied, i.e., the positioning takes place in the XY-plane, our system achieves a repeatability of $0.022\ \mathrm{mm}$. The mean repeatabilities we have calculated from our measurements are $< 0.01\ \mathrm{mm}$ for the XY plane and $< 0.02\ \mathrm{mm}$ for free space positioning.

In our laboratory applications (e.g., EIT measurements), measurements are performed with step sizes of at least $0.5\ \mathrm{mm}$. The errors caused by the inaccuracies of the positioning system are taken into account based on the determined repeatability. The repeatability of our positioning system is significantly higher than position information expected from underwater positioning systems (UPS) for real-world applications, that typically work in the range of m or cm [12], [13], [14]. For this reason, systems developed for outdoor operation e.g. at sea must be much more robust against positional uncertainties than for our research in the laboratory with our proposed positioning system.

IV. Conclusion

In this paper, we present the development of an open, scalable 3D underwater positioning system for laboratories. The systems' components enable us to resize the system, adapt the speed and resolution for dedicated research activities. We also present a remote control implemented with the MQTT protocol to perform automated, precise measurements. We evaluate the accuracy of our system with measurements applying a laser-based distance measurement as a reference. The measurement results are very promising with an a precision of better than $0.1\ \mathrm{mm}$ in most of the cases.

Although the positioning system was designed for water tanks, the flexibility and the dimensions are very well suited for experiments in indoor localization and were already used in experiments where automatic precise movement is required.

In the next step, we will build a larger variant of the system for a water tank with $3\ \mathrm{m} \times 2\ \mathrm{m} \times 1\ \mathrm{m}$.

Acknowledgments

This publication results from the research of the Center of Excellence CoSA at the Technische Hochschule Lübeck and is funded by the Federal Ministry of Economic Affairs and Energy of the Federal Republic of Germany (Id 03SX467B, Project EXTENSE, Project Management Agency: Jülich PTJ). Horst Hellbrück is an adjunct professor at the Institute of Telematics of University of Lübeck.

References

[1] G. Bouchette, P. Church, J. E. Mcfee, and A. Adler, "Imaging of compact objects buried in underwater sediments using electrical impedance tomography," *IEEE transactions on geoscience and remote sensing*, vol. 52, no. 2, pp. 1407–1417, 2013.

[2] C. Capus, Y. Pailhas, K. Brown, and D. Lane, "Detection of buried and partially buried objects using a bio-inspired wideband sonar," in *OCEANS'10 IEEE SYDNEY*. IEEE, 2010, pp. 1–6.

[3] A. Schuldei, F. John, G. Ardelt, T. Suthau, and H. Hellbrück, "Development of an Electro Impedance Tomography-based Platform for Measurement of burial Depth of Cables in Subsea Sediments," in *Oceans 2019*, 2019.

[4] F. John, R. Kusche, F. Adam, and H. Hellbrück, "Differential ultrasonic detection of small objects for underwater applications," in *Global Oceans 2020: Singapore – U.S. Gulf Coast*, Oct 2020, pp. 1–7, https://ieeexplore.ieee.org/document/9389186. [Online]. Available: http://cosa.th-luebeck.de/download/pub/john-2020-differential-ultrasonic-oceans.pdf

[5] S. H. Needs, T. T. Diep, S. P. Bull, A. Lindley-Decaire, P. Ray, and A. D. Edwards, "Exploiting open source 3d printer architecture for laboratory robotics to automate high-throughput time-lapse imaging for analytical microbiology," *PloS one*, vol. 14, no. 11, p. e0224878, 2019.

[6] G. Hillar, *MQTT Essentials - A Lightweight IoT Protocol*. Packt Publishing, 2017. [Online]. Available: https://books.google.de/books?id=40EwDwAAQBAJ

[7] D. Silva, L. I. Carvalho, J. Soares, and R. C. Sofia, "A performance analysis of internet of things networking protocols: Evaluating mqtt, coap, opc ua," *Applied Sciences*, vol. 11, no. 11, p. 4879, 2021.

[8] N. Naik, "Choice of effective messaging protocols for iot systems: Mqtt, coap, amqp and http," in *2017 IEEE international systems engineering symposium (ISSE)*. IEEE, 2017, pp. 1–7.

[9] T. Szyrowski, S. K. Sharma, R. Sutton, and G. A. Kennedy, "Developments in subsea power and telecommunication cables detection: Part 1-visual and hydroacoustic tracking." *Underwater Technology*, vol. 31, no. 3, 2013.

[10] "Keyence IL100," https://www.keyence.de/products/measure/laser-1d/il/models/il-100/, accessed: 2021-07-23.

[11] "RedPitaya fast analogue io," https://redpitaya.readthedocs.io/en/latest/developerGuide/125-14/fastIO.html, accessed: 2021-04-30.

[12] A. Alcocer, P. Oliveira, and A. Pascoal, "Study and implementation of an ekf gib-based underwater positioning system," *Control engineering practice*, vol. 15, no. 6, pp. 689–701, 2007.

[13] F. Akhoundi, A. Minoofar, and J. A. Salehi, "Underwater positioning system based on cellular underwater wireless optical cdma networks," in *2017 26th Wireless and Optical Communication Conference (WOCC)*. IEEE, 2017, pp. 1–3.

[14] M. Morgado, P. Oliveira, and C. Silvestre, "Experimental evaluation of a usbl underwater positioning system," in *Proceedings ELMAR-2010*. IEEE, 2010, pp. 485–488.